

OPEN ACCESS

Analytical modelling of acoustic emission from buried or surface-breaking cracks under stress

To cite this article: W Ben Khalifa *et al* 2012 *J. Phys.: Conf. Ser.* **353** 012016

View the [article online](#) for updates and enhancements.

You may also like

- [Feasibility study of using smart aggregates as embedded acoustic emission sensors for health monitoring of concrete structures](#)
Weijie Li, Qingzhao Kong, Siu Chun Michael Ho *et al.*
- [An integrated approach to evaluate the measurement capability and acceptability of acoustic emission sensors](#)
Haizhou Chen, Janet Lin, Nian Chen *et al.*
- [Performance monitoring of large-scale autonomously healed concrete beams under four-point bending through multiple non-destructive testing methods](#)
G Karaiskos, E Tsangouri, D G Aggelis *et al.*



ECS
The
Electrochemical
Society
Advancing solid state &
electrochemical science & technology

DISCOVER
how sustainability
intersects with
electrochemistry & solid
state science research

Analytical modelling of acoustic emission from buried or surface-breaking cracks under stress

W Ben Khalifa¹, K Jezzine¹, G Hello² and S Grondel³

¹ CEA, LIST, 91191 Gif-sur-Yvette CEDEX, France

² Laboratoire Roberval, Université de Technologie de Compiègne, Centre de Recherches de Royallieu, BP 20529, 60205 Compiègne

³ Département OAE, IEMN, UMR CNRS 8520, Université de Valenciennes et du Hainaut Cambrésis, Le Mont Houy, 59313 Valenciennes Cedex 9

E-mail: warida.ben-khalifa@cea.fr

Abstract. Acoustic emission (AE) is a non-destructive testing method used in various industries (aerospace, petrochemical and pressure-vessel industries in general, power generation, civil engineering, mechanical engineering, etc...) for the examination of large structures subjected to various stresses (e.g. mechanical loading). The energy released by a defect under stress (the AE phenomenon) can propagate as guided waves in thin structures or as surface Rayleigh waves in thick ones. Sensors (possibly permanently) are positioned at various locations on the structure under examination and are assumed to be sensitive to these waves. Then, post-processing tools typically based on signal processing and triangulation algorithms can be used to inverse these data, allowing one to estimate the position of the defect from which emanates the waves measured. The French Atomic Energy Commission is engaged in the development of tools for simulating AE examinations. These tools are based on specific models for the AE sources, for the propagation of guided or Rayleigh waves and for the behaviour of AE sensors. Here, the coupling of a fracture mechanics based model for AE source and surface/guided wave propagation models is achieved through an integral formulation relying on the elastodynamic reciprocity principle. As a first approximation, a simple piston-like model is used to predict the sensitivity of AE sensors. Predictions computed by our simulation tool are compared to results from the literature for validation purpose.

1. Introduction

Acoustic emission from a crack under stress is composed of body waves as well as surface waves in thick structures. In the case of thin structures, acoustic emission is composed of guided waves that can propagate over long distance without loss of energy.

In this paper, we consider only thick structures and we assume that only the radiated surface waves need to be considered. In the far field, surface waves dominate body waves. In a two-dimensional geometry surface waves do not decay, while body waves decay as $r^{-1/2}$. In a three-dimensional geometry, surface wave decay as $r^{-1/2}$ and body waves decay as r^{-1} , where r is the distance between the source and an observation point.

The objective is to model the acoustic emission monitoring from the propagation to the detection.

The geometry is an isotropic half space which is subjected to an arbitrary stress. We consider a two-dimensional configuration and we assume that a crack with an arbitrary orientation under stress will propagate and the released energy will produce transient surface waves.

We have, as input data, an acoustic emission model provided in the frame of the ANR project MACSIM by the University of Compiegne UTC; this fracture mechanics based model gives the evolution of the spatial-temporal elastodynamic fields (displacements and stresses) on the crack.

On the other hand we consider an analytical surface waves propagation model given by [1].

Following a method proposed by [2], the surface wave generated by acoustic emission from a crack under stress will be obtained by an application of the elastodynamic reciprocity principle. This principle can be written for a body of volume V and surface S :

$$\int_V [f_i^A u_i^B - f_i^B u_i^A] dV = \int_S [\tau_{ij}^B u_j^A - \tau_{ij}^A u_j^B] n_j dS \quad (1)$$

where n_i are the components of the outward normal to S , f_i , u_i and τ_{ij} are the components of body forces, displacements and stresses. This theorem connects two different elastodynamic states, state A and state B. We defined state A as the desired solution for the surface wave generated by a crack under stress while state B is an auxiliary solution involving a virtual surface wave.

2. Coupling of an AE model and an analytical Rayleigh wave propagation model

2.1 Rayleigh wave in 2D geometry

We consider an isotropic homogenous half-space relative to the x, z coordinate system.

In this case, the displacements and stresses of the Rayleigh wave can be written as:

$$u_x^A(x, z) = iV^R(z) \exp(-ik_R x) \quad (2)$$

$$u_z^A(x, z) = -W^R(z) \exp(-ik_R x) \quad (3)$$

$$\tau_{xx}^A(x, z) = -T_{xx}^R(z) \exp(-ik_R x) \quad (4)$$

$$\tau_{xz}^A(x, z) = iT_{xz}^R(z) \exp(-ik_R x) \quad (5)$$

$$\tau_{zz}^A(x, z) = -T_{zz}^R(z) \exp(-ik_R x), \quad (6)$$

where

$$V^R(z) = d_1 \exp(-pz) + d_2 \exp(-qz) \quad (7)$$

$$W^R(z) = d_3 \exp(-pz) - \exp(-qz) \quad (8)$$

$$T_{xx}^R(z) = \mu [d_4 \exp(-pz) + d_5 \exp(-qz)] \quad (9)$$

$$T_{xz}^R(z) = \mu [d_6 \exp(-pz) + d_7 \exp(-qz)] \quad (10)$$

$$T_{zz}^R(z) = \mu [d_8 \exp(-pz) + d_9 \exp(-qz)] \quad (11)$$

$d_1, d_2, d_3, d_4, d_5, d_6, d_7, d_8$ and d_9 are defined by:

$$d_1 = -\frac{1}{2} \frac{k_R^2 + q^2}{k_R p} \quad (12)$$

$$d_2 = \frac{q}{k_R} \quad (13)$$

$$d_3 = \frac{1}{2} \frac{k_R^2 + q^2}{k_R} \quad (14)$$

$$d_4 = \frac{1}{2} (k_R^2 + q^2) \frac{2p^2 + k_R^2 - q^2}{pk_R^2} \quad (15)$$

$$d_5 = -2q \quad (16)$$

$$d_6 = \frac{k_R^2 + q^2}{k_R p} \quad (17)$$

$$d_7 = -\frac{k_R^2 + q^2}{k_R p} \quad (18)$$

$$d_8 = -\frac{1}{2} \frac{k_R^2 + q^2}{k_R p} (k_R^2 + q^2) \quad (19)$$

$$d_9 = 2q \quad (20)$$

The quantities p and q are defined by:

$$p^2 = k_R^2 - k_l^2 \quad (21)$$

$$q^2 = k_R^2 - k_t^2 \quad (22)$$

The Rayleigh wave number is defined by $k_R = k_l / \eta_R$ where $k_t = \omega \left(\frac{\rho}{\mu} \right)^{\frac{1}{2}}$ and $k_l = \omega \left(\frac{\rho}{\lambda + 2\mu} \right)^{\frac{1}{2}}$

are the wave numbers of transverse and longitudinal bulk waves and

$$\eta_R = \frac{0.87 + 1.12\nu}{1 + \nu} \quad (23)$$

ρ , ν , λ and μ are respectively the density of the medium, Poisson ratio and the elastic Lamé constants

defined by: $\lambda = \frac{E\nu}{(1+\nu)(1-2\nu)}$ and $\mu = \frac{E}{2(1+\nu)}$, where E is the Young's modulus.

2.2. State A

We consider a crack with arbitrary orientation under an arbitrary stress. The acoustic emission from this crack will generate surface waves whose displacements and stresses can be written as:

$$u_x^A(x, z) = iA(\omega)V^R(z)\exp(\pm ik_R x) \quad (24)$$

$$u_z^A(x, z) = \pm A(\omega)W^R(z)\exp(\pm ik_R x) \quad (25)$$

$$\tau_{xx}^A(x, z) = \pm A(\omega)T_{xx}^R(z)\exp(\pm ik_R x) \quad (26)$$

$$\tau_{xz}^A(x, z) = iA(\omega)T_{xz}^R(z)\exp(\pm ik_R x) \quad (27)$$

$$\tau_{zz}^A(x, z) = \pm A(\omega)T_{zz}^R(z)\exp(\pm ik_R x) \quad (28)$$

The plus and minus signs, in equations (24)-(28), are for the propagation in the negative x direction and positive x direction and $A(\omega)$ is the amplitude of the Rayleigh wave (unknown of the radiation problem).

2.3. State B

The second state is an auxiliary solution; we define this state as a virtual surface wave that propagates in the positive x direction, in the absence of the crack, the displacements and stresses of the Rayleigh wave can be written as:

$$u_x^B(x, z) = iV^R(z)\exp(-ik_R x) \quad (29)$$

$$u_z^B(x, z) = W^R(z)\exp(-ik_R x) \quad (30)$$

$$\tau_{xx}^B(x, z) = T_{xx}^R(z)\exp(-ik_R x) \quad (31)$$

$$\tau_{xz}^B(x, z) = iT_{xz}^R(z)\exp(-ik_R x) \quad (32)$$

$$\tau_{zz}^B(x, z) = T_{zz}^R(z) \exp(-ik_R x) \quad (33)$$

2.4. Application of the elastodynamic reciprocity theorem

In equation (1), the first integral on the volume vanishes, since there are no body forces in states A and B. The reciprocity principle can be written as:

$$\int_S [\tau_{ij}^B u_j^A - \tau_{ij}^A u_j^B] n_j dS = 0 \quad (34)$$

We consider the region of the half-plane limited by the line $x=a$ and the line $x=b$. The acoustic emission source, in the half plane, is an arbitrary oriented crack. l is the final length of the crack located at v_0 with respect to the v axis of the local basis (u, v) defined in figure 2. The crack is considered as a surface of displacement and stress discontinuity evolving with time. The plane of the crack makes an angle β with the z axis. The surface S of the reciprocity problem is composed by the surface limited by the blue contour in the half-plane and the crack surface, n is the local normal to S .

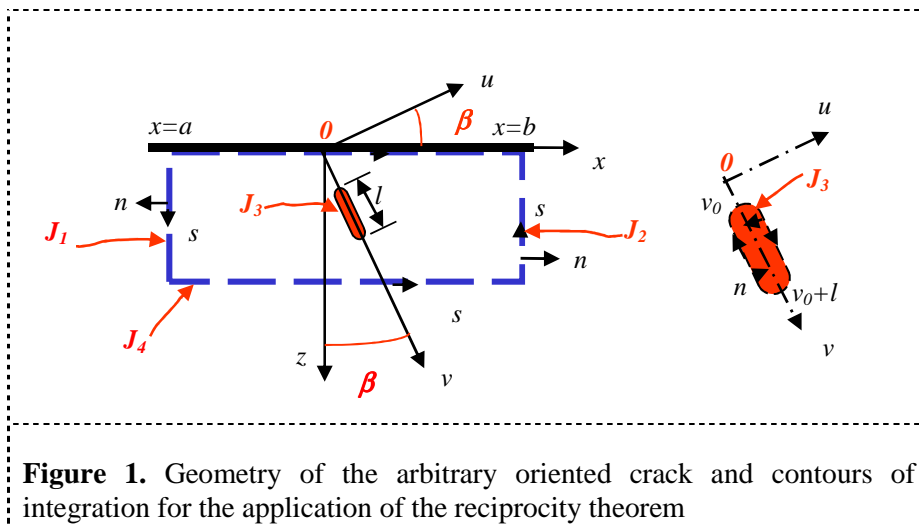


Figure 1. Geometry of the arbitrary oriented crack and contours of integration for the application of the reciprocity theorem

J_3 is the integral on the surface of the crack, J_1 is the integral along the line $x = a, 0 \leq z < \infty$, J_2 is the integral along the line $x = b, 0 \leq z < \infty$ and J_4 is the integral along the line $z = \text{constant} \rightarrow \infty$, where the amplitude of the Rayleigh wave tends to zero.

There is no contribution from the integral on the free surface and on $z = \text{constant} \rightarrow \infty$, and the integral along J_1 and J_2 only yields contributions from counter-propagating wave [3].

For $(x = b, 0 \leq z < \infty)$ we have:

$$J_2 = \int_0^\infty [\tau_{ij}^B u_i^A - \tau_{ij}^A u_i^B] \Big|_{x=b} n_i dS = 0 \quad (35)$$

Along $(x = a, 0 \leq z < \infty)$, we have:

$$J_1 = - \int_0^\infty F_{AB}(x, z) \Big|_{x=a} dz \quad (36)$$

where

$$F_{AB}(x, z) = \tau_{xx}^B u_x^A + \tau_{xz}^B u_z^A - \tau_{xx}^A u_x^B - \tau_{xz}^A u_z^B \quad (37)$$

We replace the displacements and stresses by their expressions:

$$J_1 = 2iAI \quad (38)$$

with

$$I = \int_0^\infty [T_{xx}^R(z)V^R(z) - T_{xz}^R(z)W^R(z)] dz \quad (39)$$

We divide the integral along the surface of the crack into two parts:

The first integral J_3^+ is along the line ($u=0^+$, $v_0 \leq v < v_0 + l$) and the second integral J_3^- is along the line ($u=0^-$, $v_0 \leq v < v_0 + l$).

Along ($u=0^+$, $v_0 \leq v < v_0 + l$), J_3^+ can be written as:

$$J_3^+ = - \int_{v_0}^{l+v_0} E_{AB}(u, v) \Big|_{u=0^+} dv \quad (40)$$

where

$$E_{AB}(u, v) = \tau_{uu}^B u_u^A + \tau_{uv}^B u_v^A - \tau_{uu}^A u_u^B - \tau_{uv}^A u_v^B \quad (41)$$

Along ($u=0^-$, $v_0 \leq v < v_0 + l$), J_3^- can be written as:

$$J_3^- = \int_{v_0}^{l+v_0} E_{AB}(u, v) \Big|_{u=0^-} dv \quad (42)$$

The integral along the surface of the crack can be written as

$$J_3 = J_3^+ + J_3^- = \int_{v_0}^{l+v_0} \left\{ E_{AB}(u, v) \Big|_{u=0^-} - E_{AB}(u, v) \Big|_{u=0^+} \right\} dv \quad (43)$$

$$J_3 = \int_{v_0}^{l+v_0} \left\{ -\tau_{uu}^B(u, v) \Big|_{u=0} \Delta u_u - \tau_{uv}^B(u, v) \Big|_{u=0} \Delta u_v + \Delta \tau_{uu}^A u_u^B(u, v) \Big|_{u=0} + \Delta \tau_{uv}^A u_v^B(u, v) \Big|_{u=0} \right\} dv \quad (44)$$

where

$$\Delta u_u = u_u(0^+, v) - u_u(0^-, v) \quad (45)$$

$$\Delta u_v = u_v(0^+, v) - u_v(0^-, v) \quad (46)$$

$$\Delta \tau_{uv}^A = \left[\tau_{uv}^A(0^+, v) - \tau_{uv}^A(0^-, v) \right] \quad (47)$$

$$\Delta \tau_{uv}^B = \left[\tau_{uv}^B(0^+, v) - \tau_{uv}^B(0^-, v) \right] \quad (48)$$

The amplitude of the Rayleigh wave can be calculated from equation (49):

$$J_1 + J_3 = 0 \quad (49)$$

We replace J_1 and J_3 by their expressions from equations (44) and (38):

$$2iAI = \int_{v_0}^{l+v_0} \left\{ \tau_{uu}^B(0, v) \Delta u_u + \tau_{uv}^B(0, v) \Delta u_v - \Delta \tau_{uu}^A u_u^B - \Delta \tau_{uv}^A u_v^B \right\} dv \quad (50)$$

To express the different quantities of the local basis in the global basis, we note

$$\begin{cases} C = \cos \beta \\ S = \sin \beta \end{cases} \quad (51)$$

The rotation matrix can be written as:

$$M = \begin{pmatrix} C & -S \\ S & C \end{pmatrix} \quad (52)$$

The displacements and stresses in the local crack basis are defined by:

$$\begin{pmatrix} u_u \\ u_v \end{pmatrix} = M \begin{pmatrix} u_x \\ u_z \end{pmatrix} \quad (53)$$

$$\begin{pmatrix} \tau_{uu}^B & \tau_{uv}^B \\ \tau_{vu}^B & \tau_{vv}^B \end{pmatrix} = M^{-1} \begin{pmatrix} \tau_{xx}^B & \tau_{xz}^B \\ \tau_{zx}^B & \tau_{zz}^B \end{pmatrix} M \quad (54)$$

After replacing the displacements and stresses in equation (50) we obtain:

$$2i A I = \int_{v_0}^{l+v_0} \left\{ P(0, v) \Delta u_u + Q(0, v) \Delta u_v - \Delta \tau_{uu}^A \tilde{V}(0, v) - \Delta \tau_{uv}^A \tilde{W}(0, v) \right\} dv \quad (55)$$

where

$$P = [C^2 T_{xx}^R + 2CSiT_{xz}^R + S^2 T_{zz}^R] e^{ik_R S v} \quad (56)$$

$$Q = [-CS T_{xx}^R + (C^2 - S^2)iT_{xz}^R + SC T_{zz}^R] e^{ik_R S v} \quad (57)$$

$$\tilde{V} = [-SiV + CW] e^{ik_R S v} \quad (58)$$

$$\tilde{W} = [-SiV + CW] e^{ik_R S v} \quad (59)$$

The amplitude of the emitted Rayleigh wave is:

$$A = \frac{-i}{2I} \int_{v_0}^{l+v_0} \left\{ P(0, v) \Delta u_u + Q(0, v) \Delta u_v - \Delta \tau_{uu}^A \tilde{V}(0, v) - \Delta \tau_{uv}^A \tilde{W}(0, v) \right\} dv \quad (60)$$

In the case of a tensile stress crack the amplitude of the Rayleigh wave can be written as:

$$A = \frac{-i}{2I} \int_{z_0}^{l+z_0} \left\{ T_{xx}(0, z) \Delta u_x \right\} dz \quad (61)$$

By substituting A in equations (24) and (25), the displacement components at $z=0$ are :

$$u_z^A(x, z_1) = \pm \frac{-i}{2I} \int_{z_0}^{l+z_0} \left\{ T_{xx}(0, z) \Delta u_x \right\} dz W^R(z_1) \exp(\pm ik_R x) \quad (62)$$

$$u_x^A(x, z_1) = \frac{1}{2I} \int_{z_0}^{l+z_0} \left\{ T_{xx}(0, z) \Delta u_x \right\} dz V^R(z_1) \exp(\pm ik_R x) \quad (63)$$

As it is shown by Achenbach, this result is equivalent to the displacement due to the presence of a distribution of dipoles along $z_0 \leq z \leq z_0 + l$ [4]

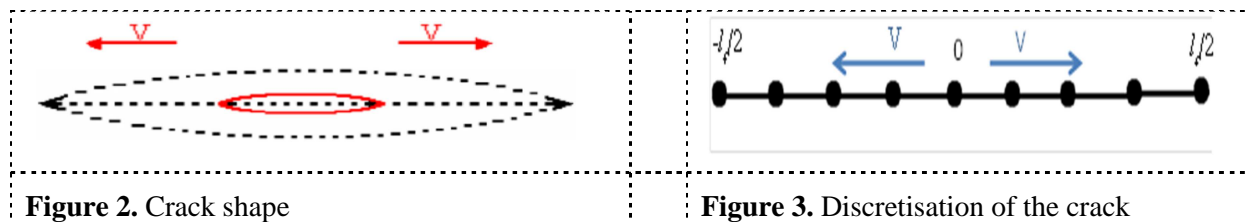
2.5. Acoustic emission source

The COD (crack opening displacement) for a crack of length $2a$ along the z axis subjected to uniaxial tension σ^∞ is:

$$\Delta u_x(z) = \sigma^\infty \frac{\kappa+1}{4\mu} \sqrt{a^2 - z^2} \quad (64)$$

where $\kappa = (3 - 4\nu)$ in the case of plane strain.

We consider a crack of length l subjected to uniaxial tension, figure 2 shows the crack shape. We discretise the crack as shown in figure 3.



We assume that the crack length evolves from $l_0 = 1\text{mm}$ to $l = 5\text{mm}$ at a velocity V during $T = 0.8\mu\text{s}$, we consider a sampling frequency $F_e = 50\text{MHz}$.

We define z_j and t_n as:

$$z_j = jV\Delta t \quad (65)$$

$$t_n = t_0 + n \frac{1}{F_e} \quad (66)$$

j varies from $-H/2$ to $H/2$, and n varies from 0 to N where:

$$\Delta t = 1/F_e \quad (67)$$

$$N = \frac{T}{\Delta t} \quad (68)$$

$$H = \frac{l}{V\Delta t} \quad (69)$$

Equation (64) can be discretised as follows:

$$\Delta u_x(z_j, t_n) = \sigma^\infty \frac{\kappa+1}{4\mu} \sqrt{((l_0 + nV\Delta t)/2)^2 - z_j^2} \quad (70)$$

for $|z_j| \leq (l_0 + nV\Delta t)/2$

$$\Delta u_x(z_j) = 0 \quad (71)$$

for $(l_0 + nV\Delta t)/2 \leq |z_j| \leq l/2$

We take the Fourier transform of the COD to obtain the displacement and stress fields of the emitted Rayleigh wave in the frequency domain.

Displacement and stress fields in the time domain are obtained by the inverse Fourier Transform.

3. Simulation and comparison with literature

We have simulated the acoustic emission from a buried crack under a uniform stress with different crack propagation velocities V (500m/s, 1000m/s, 2000m/s and 2500m/s). We assume that the crack, of final length l located at a distance d from the free surface, propagates at a velocity V and the crack length evolves from 1mm to 5mm under 200 MPa.

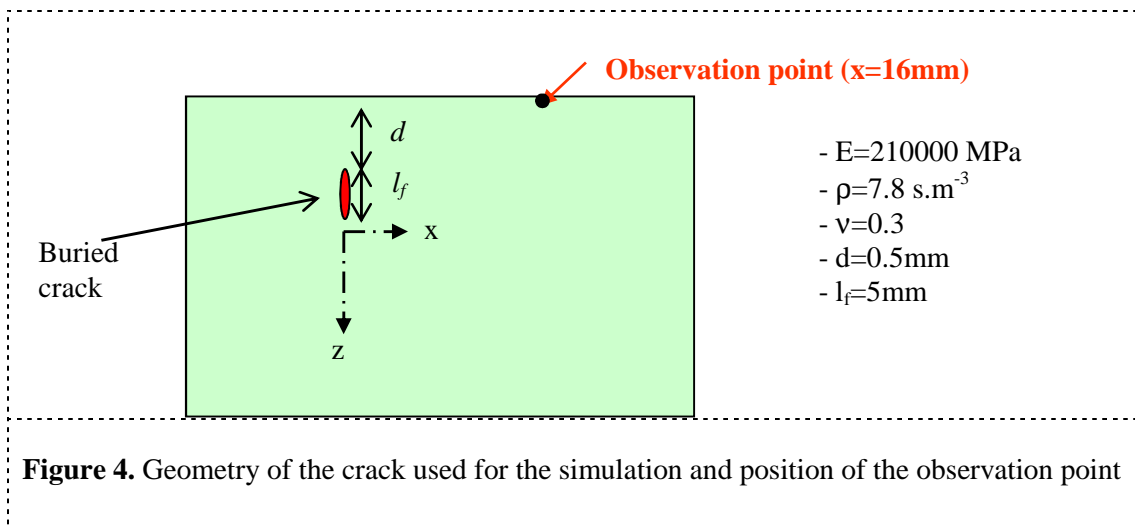


Figure 4. Geometry of the crack used for the simulation and position of the observation point

Figure 5 to 8 show the evolution of the crack opening displacement, obtained from the fracture mechanics based crack model, at different propagation times ($t=0\mu\text{s}$, $t=0.2\mu\text{s}$, $t=0.4\mu\text{s}$ and $t=0.8\mu\text{s}$) with a constant crack-tip velocity $V=2500\text{m/s}$.

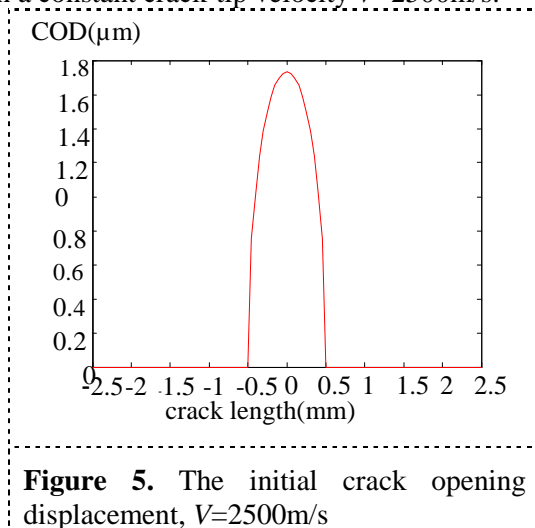


Figure 5. The initial crack opening displacement, $V=2500\text{m/s}$

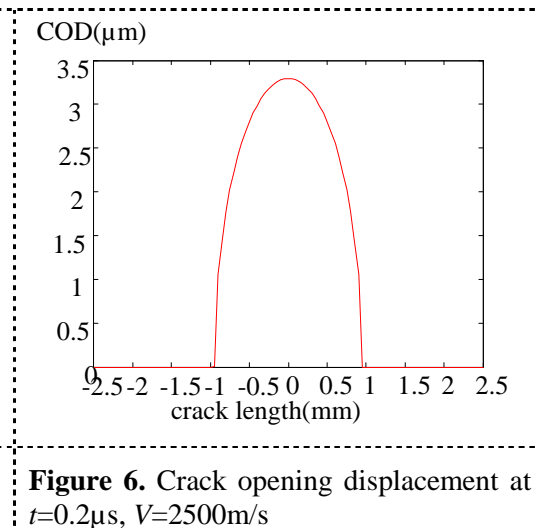


Figure 6. Crack opening displacement at $t=0.2\mu\text{s}$, $V=2500\text{m/s}$

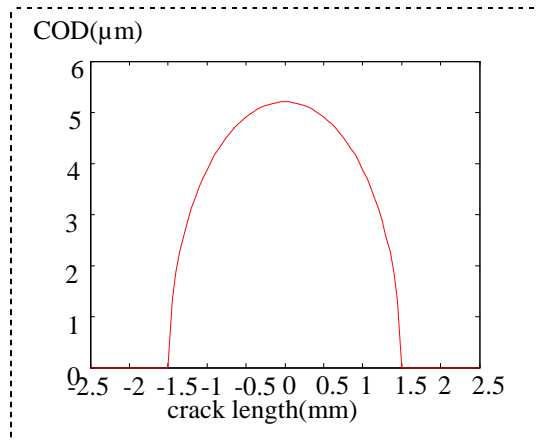


Figure 7. Crack opening displacement at $t=0.4\mu\text{s}$, $V=2500\text{m/s}$

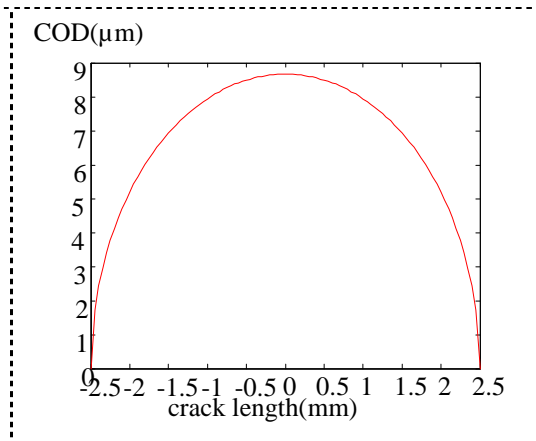


Figure 8. Crack opening displacement at $t=0.8\mu\text{s}$, $V=2500\text{m/s}$

The normal displacement of the emitted wave was simulated with different crack-tip speeds. Figure 9 to 12 shows the influence of the crack propagation speed on the wave front and the Rayleigh wave arrival time.

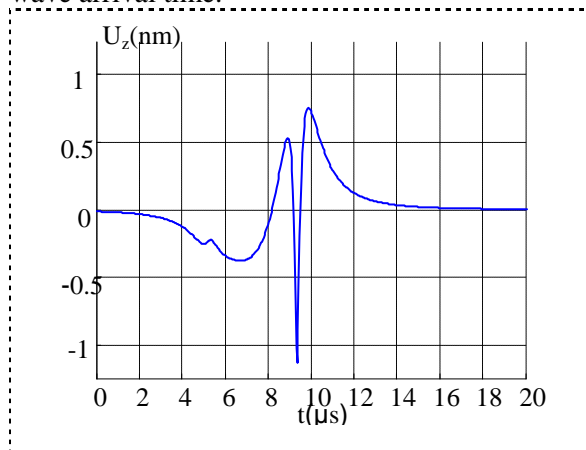


Figure 9. Surface normal displacement in nm at $x=16\text{mm}$, $V=500\text{m/s}$

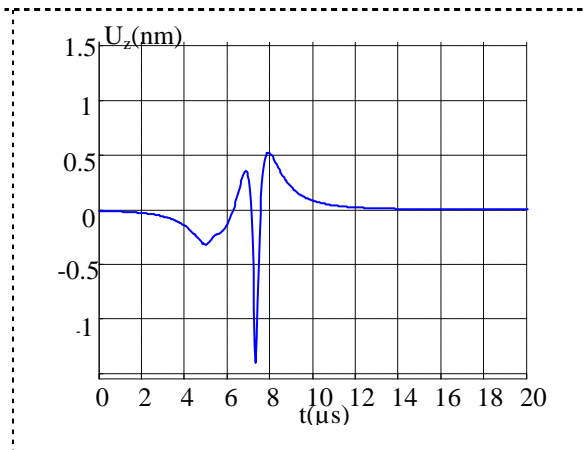


Figure 10. Surface normal displacement in nm at $x=16\text{mm}$, $V=1000\text{m/s}$

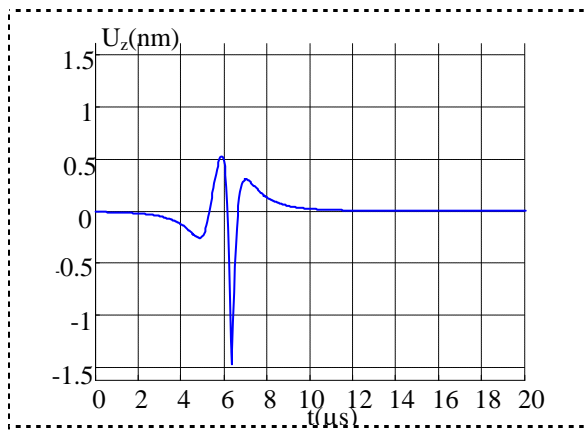


Figure 11. Surface normal displacement in nm at $x=16\text{mm}$, $V=2000\text{m/s}$

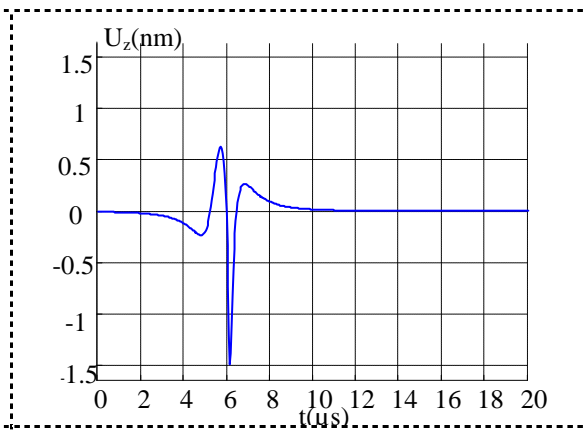


Figure 12. Surface normal displacement in nm at $x=16\text{mm}$, $V=2500\text{m/s}$

Harris *et al.* [5] developed an analytical model for acoustic emission from a buried crack in which he takes into account the displacement and the velocity of the crack-tip. He used an approximation of the Fourier transform near the arrival time of the Rayleigh wave. Figure 13 shows the approximation of the normalized Rayleigh wave velocity near the arrival time of the Rayleigh wave obtained by [5].

In figure 14 we present the simulation of the Rayleigh wave velocity emitted by a crack with the same length and location. Our 2D source model (the crack is considered infinite in the y direction) takes into account the crack opening displacement at all the points of the crack along its length, whereas the 3D model presented in [5] is a circular crack and it is based on the displacement at small distances ahead of the original crack tip.

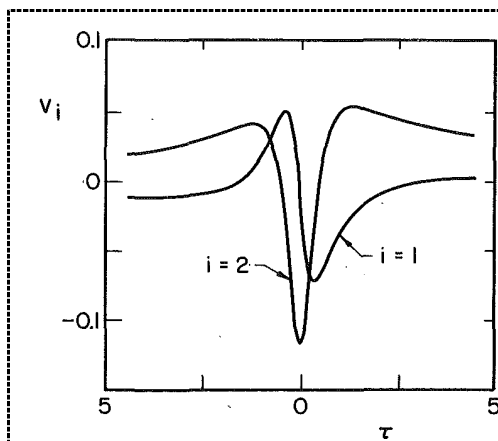


Figure 13. Normalised Rayleigh wave particle velocity v_i from [5] as a function of the normalized time τ , $i=2$ corresponds to the vertical velocity and $i=1$ corresponds to the horizontal velocity, $\tau=t/(d/v_R)-x/d$

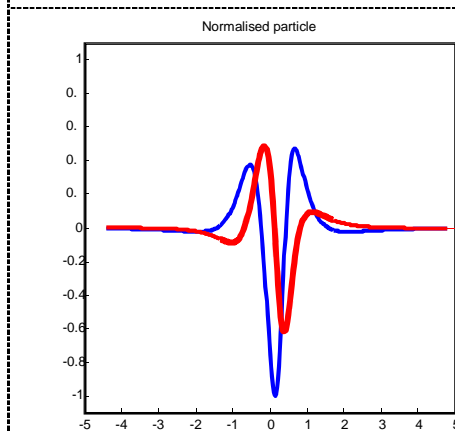


Figure 14. Normalised Rayleigh wave particle velocity, $V=1666\text{m/s}$

For these reasons, we can compare our simulation, only qualitatively, with the results of Harris *et al.* We notice that the curves are similar near $\tau=0$. The difference is due to the dimension of the AE source model and the propagation model (3D or 2D), to the fracture mechanic solution of the crack problem asymptotic solution used by [5] or analytical solution used in our formulation. In addition, curves in figure 13 are computed with the approximation of the Fourier transform near the arrival time of the Rayleigh wave.

A 3D Rayleigh wave model is under development, this model will take into account a 3D AE source model.

4. Example of application

We have simulated the reception by an AE sensor; we use a piston-like model as a first approximation, in which we take into account only the normal velocity of the Rayleigh wave.

In the case of a 2D piston-like model, corresponding to a rectangular transducer whose width is considered infinite, the delivered voltage can be written as [6]:

$$E_{0R} = \frac{1}{L} \int_0^L v_z(x) m(x) dx \tag{62}$$

where L is the length of the transducer, v_z is the vertical velocity of the Rayleigh wave and m the spatial sensibility.

We consider transducer with 10mm length and a constant spatial sensibility $m(x) = 1$, placed at a distance of 100mm from the plane of the crack as shown in figure 13.

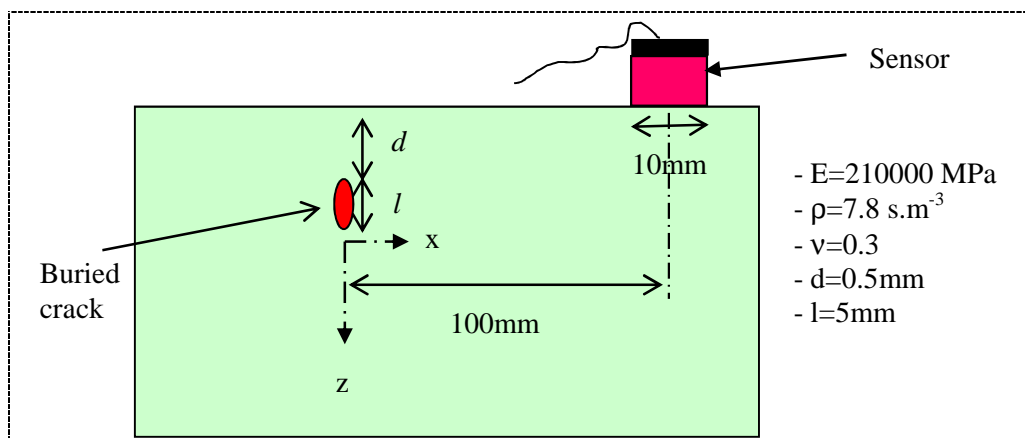


Figure 15. Definition of the crack and the sensor positions

The delivered voltage by the transducer is presented in figure 16.

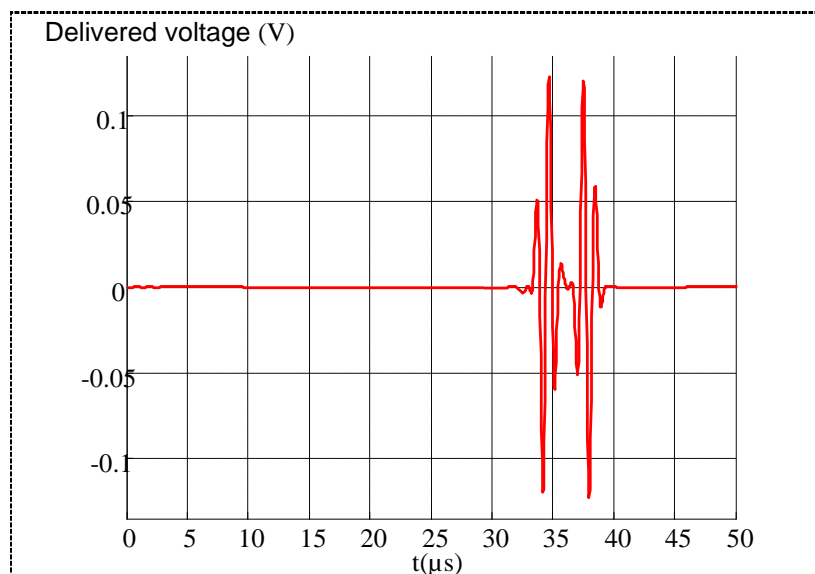


Figure 16. Delivered voltage by the AE sensor after the acoustic emission of the Rayleigh wave ($V=1666\text{m/s}$).

The delivered voltage signal comprises two waveforms which correspond to the difference between the phase terms at the ends of the transducer. In equation (62) the integral is reduced to an integral along the transducer length and to a simple difference of the exponential terms at the transducer ends.

5. Conclusion

The Rayleigh wave emitted by a crack under stress was simulated in the far field. In fact, the surface wave is the dominant disturbance because of its slower geometrical decay rate.

We have shown that the Rayleigh wave displacement depends on the crack-tip speed.

Simulation of the AE of the Rayleigh wave shows the influence of the AE source model on the prediction of the emitted wave. We have compared qualitatively our simulation with the result of Harris *et al.* The differences between the results can be explained by the dimension of the acoustic source and propagation models, the fracture mechanic solutions and the Fourier transform approximation near the Rayleigh wave arrival time. The delivered voltage at a transducer output was simulated with a piston-like model, as a first approximation, considering only the surface normal displacement of the Rayleigh wave.

Because of their thicknesses, AE sensors present also radial modes and this will be simulated by finite elements in order to take into account the radial displacements of the Rayleigh wave in addition to the vertical displacements. Results will be compared with those obtained with the piston-like model.

Acoustic emission from crack under stress in 3D geometry will be modeled using a virtual cylindrical surface wave.

6. Acknowledgement

G. Hello's work concerning the acoustic emission source model was supported by the ANR in the frame of the project MACSIM ANR-08-COSI-005-01.

References

- [1] Viktorov I A 1967 *Rayleigh and Lamb waves* (New York: Plenum Press)
- [2] Achenbach J D 2008 Acoustic emission from a surface-breaking crack under cyclic loading *Acta Mech* **195** 61
- [3] Achenbach J D 2003 *Reciprocity in elastodynamics* (Cambridge: Cambridge University Press)
- [4] Achenbach J D 2005 Combination of a virtual wave and the reciprocity theorem to analyse surface wave generation on a transversely isotropic solid *Philosophical Magazine* **85** 4143
- [5] Harris J G and Pott J 1984 Surface motion excited by acoustic emission from a buried crack *J. Appl. Mech.* **51** 77
- [6] Goujon L and Baboux J C 2003 Behaviour of acoustic emission sensors using broadband calibration techniques *Meas. Sci. Technol.* **14** 903